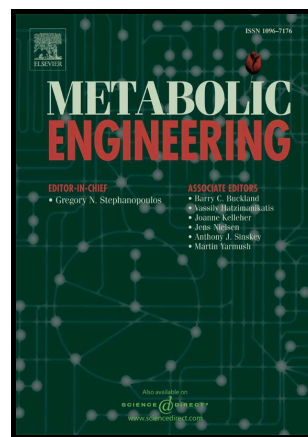


Systems-level engineering and characterization of *Clostridium autoethanogenum* through heterologous production of poly-3-hydroxybutyrate (PHB)

Renato de Souza Pinto Lemgruber, Kaspar Valgepea, Ryan Tappel, James B. Behrendorff, Robin William Palfreyman, Manuel Plan, Mark P. Hodson, Séan Dennis Simpson, Lars K. Nielsen, Michael Köpke, Esteban Marcellin



PII: S1096-7176(18)30375-6
DOI: <https://doi.org/10.1016/j.ymben.2019.01.003>
Reference: YMBEN1508

To appear in: *Metabolic Engineering*

Received date: 27 September 2018
Revised date: 3 January 2019
Accepted date: 5 January 2019

Cite this article as: Renato de Souza Pinto Lemgruber, Kaspar Valgepea, Ryan Tappel, James B. Behrendorff, Robin William Palfreyman, Manuel Plan, Mark P. Hodson, Séan Dennis Simpson, Lars K. Nielsen, Michael Köpke and Esteban Marcellin, Systems-level engineering and characterization of *Clostridium autoethanogenum* through heterologous production of poly-3-hydroxybutyrate (PHB), *Metabolic Engineering*, <https://doi.org/10.1016/j.ymben.2019.01.003>

This is a PDF file of an unedited manuscript that has been accepted for publication. As a service to our customers we are providing this early version of the manuscript. The manuscript will undergo copyediting, typesetting, and review of the resulting galley proof before it is published in its final citable form. Please note that during the production process errors may be discovered which could affect the content, and all legal disclaimers that apply to the journal pertain.

Systems-level engineering and characterization of *Clostridium autoethanogenum* through heterologous production of poly-3-hydroxybutyrate (PHB)

Renato de Souza Pinto Lemgruber^{a1}, Kaspar Valgepea^{a,12}, Ryan Tappel^b, James B. Behrendorff^{b3}, Robin William Palfreyman^a, Manuel Plan^{a,c}, Mark P. Hodson^{a,c4}, Séan Dennis Simpson^b, Lars K. Nielsen^{a,c}, Michael Köpke^b, Esteban Marcellin^{a,c*}

^aAustralian Institute for Bioengineering and Nanotechnology (AIBN), The University of Queensland, Brisbane, QLD 4072, Australia

^bLanzaTech Inc., Skokie, IL 60077, USA

^cMetabolomics Australia, AIBN, The University of Queensland, Brisbane, Australia

renato.lemgruber@uq.edu.au

k.valgepea@uq.edu.au

Ryan.Tappel@lanzatech.com

jbe@plen.ku.dk

r.palfreyman@uq.edu.au

m.plan@uq.edu.au

m.hodson@victorchang.edu.au

sean@lanzatech.com

lars.nielsen@uq.edu.au

Michael.Koepke@lanzatech.com

e.marcellin@uq.edu.au

*Corresponding author.

¹ These authors contributed equally to this work.

² Present address: Institute of Technology, University of Tartu, Tartu, Estonia

³ Present address: Copenhagen Plant Science Centre, Department of Plant and Environmental Sciences, University of Copenhagen, 1871 Frederiksberg C, Denmark

⁴ Present address: Victor Chang Cardiac Research Institute, Lowy Packer Building, 405 Liverpool St, Darlinghurst, NSW 2010, Australia

Abstract

Gas fermentation is emerging as an economically attractive option for the sustainable production of fuels and chemicals from gaseous waste feedstocks. *Clostridium autoethanogenum* can use CO and/or CO₂ + H₂ as its sole carbon and energy sources. Fermentation of *C. autoethanogenum* is currently being deployed on a commercial scale for ethanol production. Expanding the product spectrum of acetogens will enhance the economics of gas fermentation. To achieve efficient heterologous product synthesis, limitations in redox and energy metabolism must be overcome. Here, we engineered and characterised at a systems-level, a recombinant poly-3-hydroxybutyrate (PHB)-producing strain of *C. autoethanogenum*. Cells were grown in CO-limited steady-state chemostats on two gas mixtures, one resembling syngas (20% H₂) and the other steel mill off-gas (2% H₂). Results were characterized using metabolomics and transcriptomics, and then integrated using a genome-scale metabolic model reconstruction. PHB-producing cells had an increased expression of the Rnf complex, suggesting energy limitations for heterologous production. Subsequent optimization of the bioprocess led to a 12-fold increase in the cellular PHB content. The data suggest that the cellular redox state, rather than the acetyl-CoA pool, was limiting PHB production. Integration of the data into the genome-scale metabolic model showed that ATP availability limits PHB production. Altogether, the data presented here advances the fundamental understanding of heterologous product synthesis in gas-fermenting acetogens.

Keywords

Acetogens; Wood-Ljungdahl pathway; Polyhydroxyalkanoate; Gas fermentation; *C. autoethanogenum*; PHB

1. Introduction

There is an imperative need to decrease our dependency on fossil fuels (Friedlingstein et al., 2014; McGlade and Ekins, 2015) and gas fermentation has emerged as a promising alternative for the sustainable production of fuels and chemicals (Daniell et al., 2012; Liew et al., 2016). Gas fermentation enables the capture and recycling of waste carbon – in the form of carbon monoxide (CO) and carbon dioxide (CO₂) – while not competing for arable land (Daniell et al., 2012; Munasinghe and Khanal, 2010). C₁ gases are low-cost feedstocks, readily available as industrial waste products (e.g. from steel production) or from gasification of municipal and agricultural waste (Daniell et al., 2012; Liew et al., 2016; Munasinghe and Khanal, 2010). Gas fermentation using acetogens relies on the Wood-Ljungdahl pathway (WLP) (Ragsdale and Pierce, 2008; Wood, 1991), which enables the use of CO and/or CO₂ (with H₂) as the sole carbon and redox sources to convert gases into liquids (e.g. acetate, ethanol, butanol or 2,3-butanediol) (Daniell et al., 2012; Drake et al., 2006; Liew et al., 2016; Munasinghe and Khanal, 2010).

Although genetic tools (Bengelsdorf et al., 2016; Heap et al., 2010, 2007; Huang et al., 2016; Köpke et al., 2010) and genome-scale metabolic model reconstructions (GEM) have become available for acetogens (Islam et al., 2015; Marcellin et al., 2016; Nagarajan et al., 2013), there are few metabolic engineering studies that expand the portfolio of non-native products during autotrophic growth. Furthermore, none of the engineered strains have been characterized at a systems level (Liew et al., 2016; Molitor et al., 2017). *Clostridium autoethanogenum* is a promising biocatalyst for industrial gas fermentation (Liew et al., 2016) and recent systems-level studies have compared heterotrophic and autotrophic growth (Marcellin et al., 2016), searched for alternative routes to boost ATP production (Valgepea et al., 2017b), and characterised steady-state metabolism under various autotrophic conditions (Martin et al., 2015; Valgepea et al., 2018, 2017a). Together these studies have provided

quantitative links between carbon, energy, and redox metabolism, and shed light on the regulation of acetogen metabolism. Importantly, these studies have suggested that energy and redox are tightly linked and control product formation. To further explore redox and energy metabolism in heterologous production, we performed a systems-level characterisation of a poly-3-hydroxybutyrate (PHB)-producing *C. autoethanogenum* strain in autotrophic continuous cultures.

We chose to engineer *C. autoethanogenum* for PHB production for the following reasons: 1) PHB is a polyhydroxyalkanoate (PHA) that can be used as a biodegradable polymer for the sustainable replacement of fossil fuel-based plastics; 2) PHB is non-native to acetogens and requires only three genes for heterologous production; 3) PHB is synthesised from acetyl-CoA through a linear pathway that does not directly require ATP (Peoples and Sinskey, 1989a, 1989b; Steinbüchel and Schlegel, 1991). To this end, the PHB pathway from *Cupriavidus necator* (formerly known as *Ralstonia eutropha* (Vandamme and Coenye, 2004)) was engineered into *C. autoethanogenum* as a model for heterologous production. The PHB and empty plasmid (EP) strains were tested in autotrophic continuous cultures under various bioprocess conditions, which eventually led to a 12-fold increase in the cellular PHB content. Systems-level analysis showed that heterologous production is likely limited by the ATP supply and redox rather than the acetyl-CoA pool. The data presented here advances the fundamental understanding of heterologous product synthesis in gas-fermenting acetogens.

2. Materials and Methods

The bacterial strain, growth medium, fermentation conditions, off-gas analysis, extra- and intracellular metabolomics, transcriptomics, production rates, carbon balance, and the genome-scale metabolic modelling approach used in this work are described in detail elsewhere (Valgepea et al., 2017a), and only modifications are described below.

2.1 Bacterial strain

A derivative of the *Clostridium autoethanogenum* DSM 10061 strain – DSM 19630 – was transformed with a plasmid (Heap et al., 2009) bearing the PHB pathway genes from *Cupriavidus necator* (formerly known as *Ralstonia eutropha*) under control of the promoter of the native WLP, termed hereafter “PHB strain”. The plasmid was constructed as follows: PHB pathway (Figure 1A) genes *phaA* (encoding a 3-ketothiolase enzyme that condenses two molecules of acetyl-CoA to form acetoacetyl-CoA, Genbank accession number: WP_010810132.1), *phaB* (encoding an NADPH-dependent acetoacetyl-CoA reductase that catalyses 3-hydroxybutyryl-CoA synthesis, WP_010810131.1), and *phaC* (encoding a PHA synthase that catalyses PHB polymerization, WP_013956451.1) were codon-optimized using an in-house algorithm, and synthesized as a single tricistronic operon with ribosome binding sites preceding each gene (GenScript, Piscataway, NJ). The PHB operon was placed under control of the native WLP promoter by cloning it into the previously-described pMTL83157 plasmid via GeneArt Seamless cloning (ThermoFisher Scientific). The DSM 19630 strain was also transformed with the same pMTL83157 empty plasmid, termed hereafter “Empty plasmid (EP)” strain. See Supplementary Table S1 for plasmid sequences and Supplementary Files 2 and 3 for Genbank files of the empty plasmid and PHB plasmid, respectively.

2.2 Growth medium

In addition to the previously described components of the chemically defined growth medium (Valgepea et al., 2017a), the medium also contained 15 mg/L of the antibiotic thiamphenicol added from a stock solution prepared in 50% ethanol, resulting in 0.8 g/L of ethanol in the continuous culture feed medium. The feed ethanol concentration was taken into account in all subsequent calculations.

2.3 Growth conditions

Pre-cultures were started by inoculating glycerol stocks (stored at -80 °C) into serum bottles with headspace pressurized to 190 kPa of the respective gas mix (e.g. syngas for bioreactor syngas cultures); cells were then transferred at OD 0.5-0.6 (mid-exponential growth) into Schott bottles with headspace pressurized to 140 kPa (same gas as first pre-culture) that were next used to inoculate bioreactors at OD 0.4-0.5 (mid-exponential growth). The PETC-MES medium specified in Valgepea *et al* (2017b) was used for the pre-cultures with the addition of 1.5 g/L yeast extract.

Cells were grown in bioreactors under anaerobic conditions at 37 °C, pH of 5, gas flow of 43.5 mL/min, and various agitation rates (see below) on chemically defined medium in chemostat continuous cultures (see Valgepea *et al* (2017a) for details). Two biological replicate steady-state cultures for each strain and experimental condition were achieved after three volume changes at a dilution rate of 1 day⁻¹.

2.3.1 PHB and EP experiments

We first evaluated growth of the PHB strain compared to the EP using a gas mix with 20% H₂ that resembles syngas (50% CO, 20% CO₂, 20% H₂, 10% Argon; BOC Australia), termed as conditions “PHB20” and “EP20”, respectively. Then the growth of the two strains was compared with a gas mix of 2% H₂ resembling steel mill off-gas (50% CO, 20% CO₂, 20% H₂, 10% Argon; BOC Australia), termed as conditions “PHB2” and “EP2” respectively. These gas mixes were chosen as they resemble the composition of two of the currently most relevant gaseous feedstocks for industrial-scale gas fermentation. Steady-state biomass concentrations of the cultures (grams of dry cell weight per litre - gDCW/L) at an agitation rate of 500 RPM were: PHB20 0.45 ± 0.01 (average ± standard error); PHB2 0.44 ± 0.02; EP20 0.45 ± 0.01; EP2 0.36 ± 0.01.

2.3.2 PHB-only experiments

In addition to the control condition (PHB20), three other experimental conditions were tested using the PHB strain grown on syngas by changing the noted parameter compared to the PHB20 (above). Experiment 1, named “PHB C/N ratio” (PHBC/N), had a 25-times increased carbon-to-nitrogen ratio achieved by decreasing the amount of nitrogen in the chemically defined medium 25 times and using NaOH rather than NH_4OH used in the other experiments to maintain a constant pH. Experiment 2, named “PHB Low Biomass” (PHBLowB), had a 3-times lower steady-state biomass concentration achieved with culture agitation at 250 RPM. Experiment 3, named “PHBpH5.5”, had a culture pH of 5.5. For the latter experiment, the agitation was changed (to 505 RPM) to achieve a biomass concentration and by-product inhibition similar to PHB20 and PHBC/N, as we have previously shown it has a strong effect on metabolism (Valgepea et al., 2017a). Steady-state biomass concentrations (gDCW/L) of the cultures were: PHBC/N 0.44 ± 0.01 ; PHBLowB 0.14 ± 0.01 ; PHBpH5.5 0.44 ± 0.04 .

2.4 Intracellular metabolome analysis

Concentrations of tetrahydrofolate (THF) intermediates (WLP metabolites) were determined as described previously (de Souza Pinto Lemgruber et al., 2018). Intracellular concentrations for all the other reported metabolites were determined as described previously (Valgepea et al., 2017a) except that 25 mL samples were drawn from steady-state cultures.

2.5 PHB analysis

Analysis of cellular PHB content was based on the method of (Karr et al., 1983). 25 mL samples of culture were pelleted by immediate centrifugation ($5,000 \times g$ for 10 min at 4 °C), rinsed with 5 mL of milli-Q water, and centrifuged again. Pellets were stored at -80 °C until further analysis. Pellets were then freeze-dried and weighed. Next, 1 mL of concentrated sulphuric acid was added to the pellet and PHB was acid-hydrolysed to crotonic acid for 1 h

at 90 °C. Subsequently, 4 mL of 0.014 N sulphuric acid was added and the samples were filtered using a 0.22 µm filter (Merck Millipore).

Adipic acid was added in 1:1 to the sample (400 mg/L final concentration) and used as an internal standard in HPLC analysis. For this, 30 µL of sample was injected into an Agilent Hipler H column (300 x 7.7 mm, PL1170-6830) with a guard cartridge (SecurityGuard Carbo-H, 4 X 3 mm, Phenomenex PN: AJO-4490) using an Agilent 1200 HPLC system equipped with high-performance autosampler (Agilent HiP-ALS SL, G1367C), binary pump (Agilent Bin Pump, G1312A), degasser (Agilent Degasser, G1379B), thermostatted column compartment (Agilent TCC, G1316B), multi-wavelength (Agilent MWD, G1365B) and refractive index (Agilent RID, G1362A) detectors. Analytes were eluted with 4 mM sulphuric acid at 0.6 mL/min flow rate, column temperature of 65 °C, and monitored at 210 nm UV and positive polarity at 40 °C on the RID, over an isocratic run of 30 min. Crotonic acid (Sigma #113018) was used as the standard for quantification. Peak areas were integrated using ChemStation (Rev B.03.02[341]). The PHB cellular content in grams of PHB per gDCW (PHB%) was calculated using the determined crotonic acid concentration in the sample (based on Karr et al. 1983) and the biomass concentration of the culture.

2.6 Transcriptome and metabolome data analysis

Analysis of transcriptome data from RNA sequencing was based on a previously published R-script (Valgepea et al., 2017a) with the following modifications: use of the *C. autoethanogenum* NCBI reference sequence CP006763.1 and its annotated genome described in Brown *et al* (2014); addition of the nucleotide sequence for the three aforementioned PHB genes (Supplementary Table S1).

A metabolomics package available in R (Livera and Bowne, 2014) was used to perform the statistical analysis of the intracellular metabolomics data. This script normalizes

and integrates the metabolomics data into a linear model fit (De Livera et al., 2012). Intracellular metabolite concentrations were normalised per biomass ($\mu\text{mol/gDCW}$) prior to importing the data into the script (Supplementary Tables S2 and S3). A linear model fit using ordinary statistics (i.e. non-Bayesian) was used for the statistical analysis of the metabolome data (De Livera et al., 2013, 2012).

The R-scripts used for transcriptomics and metabolomics data analysis including complete details of the methodologies and can be downloaded as Supplementary Files 4 and 5, respectively.

2.7 Genome-scale metabolic modelling

The genome-scale metabolic model GEM iCLAU786 (Valgepea et al., 2017a) was used with the addition of reactions for *phaA* (rxn00178_c0) and *phaB* (rxn01452_c0) (Figure 1A), PHB polymerization (“PHB_polymer”) and excretion (“EX_PHB”). The network’s reaction stoichiometries are specified in Supplementary Tables S4 and S6. The metabolic model together with specific constraints for each simulation can be found in Supplementary File 6. Simulations were performed for the PHB strain grown on syngas in all four conditions listed above with the results identified as SIMx in the text (e.g., SIM1) and presented in Supplementary Tables S4 and S5.

To estimate experimental metabolic flux patterns (SIM 1-8), the GEM was constrained using gas uptake and production, cysteine and ethanol uptake, by-product secretion and cellular specific growth rate, and using the maximisation of ATP dissipation as the objective function in FBA calculations, as reported previously (Valgepea et al., 2017a).

To evaluate potential limitations in cofactor supply for PHB production, we first simulated the maximal PHB production using experimental data (“control”) by constraining the GEM with measured substrate uptake rates, the specific growth rate, the maintenance ATP costs calculated above, and using maximisation of PHB yield as the objective function

in FBA calculations (SIM 9-16). Next we evaluated which single cofactor might limit PHB production in acetogens (simulations termed “single limitation”, SIM 17-48). In these simulations, SIMs 9-16 were repeated with the addition of a fixed uptake rate of either ATP, NADH, NADPH, or reduced ferredoxin (Fd_{red}) (each of these metabolites fixed at 2 mmol/gDCW/h, the maximum value where growth was feasible across all experiments, determined by increasing the uptake rate with an increment of 0.01 mmol/gDCW/h until a solution in FBA could not be found). Because SIMs 17-48 indicated that increased ATP supply led to the highest increase in PHB production (see text), we further tested which paired cofactor combination together with ATP would improve PHB the most (SIM 49-72) by fixing the uptake rate of ATP and one of the other aforementioned cofactors at the same value (simulations termed “double limitation”).

3. Results

To understand changes in redox and energy metabolism as a response to the production of PHB, *C. autoethanogenum* was engineered with PHB pathway genes from *C. necator* (PHB strain). The PHB strain was compared to an empty plasmid strain (EP) in autotrophic steady-state chemostat cultures (dilution rate of 1 day⁻¹) using a chemically defined medium. Two synthetic gas mixtures, resembling syngas (50% CO, 20% CO₂ and 20% H₂, and argon) or steel mill off-gas (50% CO, 20% CO₂ and 2% H₂, and nitrogen), were used.

3.1 Expression of the PHB pathway affects energy and redox metabolism

We first compared PHB production between growth on syngas and steel mill off-gas because substrate (H₂ in this case) and product availability change acetogen energy and redox metabolism (Marcellin et al., 2016; Schuchmann and Müller, 2014; Valgepea et al., 2017a).

Higher supply of H₂ using syngas could provide extra reducing power (Valgepea et al., 2018). As expected, the transcriptome and metabolome of the PHB strain differed from the EP strain. Although arginine was not supplied, we observed an upregulation of the arginine deiminase pathway (q-value <0.01), an alternative route found to provide ATP in acetogens (Valgepea et al., 2017b): arginine deiminase (CAETHG_3021, ~7 fold); ornithine carbamoyltransferase (CAETHG_3022, ~6 fold); carbamate kinase (CAETHG_3025, ~3.3 fold). Additionally, three genes encoding the multi-subunit Fd-NAD⁺ oxidoreductase Rnf complex that generates the proton motive force to drive the ATPase in *C. autoethanogenum* (Hess et al., 2016; Tremblay et al., 2012) showed an increase of around two-fold in the PHB strain: (CAETHG_3231, q-value=0.02; CAETHG_3228, q-value=0.04 and CAETHG_3230, q-value=0.03). These observations highlight changes in energy metabolism due to the heterologous PHB production. In addition, expression of two genes of the Wood-Ljungdahl pathway (WLP) encoding for the CO dehydrogenase/acetyl-CoA synthase (CAETHG_1610, ~1.4 fold, q-value=0.02; CAETHG_1611, 1.2 fold, q-value=0.047) and a gene encoding a (FeFe)-hydrogenase (CAETHG_1691, ~2.5 fold, q-value<0.01) were upregulated in the PHB strain. These changes may reflect the increase needed for the production of acetyl-CoA and NADPH for PHB production (Figure 1A; Supplementary Table S7).

At the metabolome level, the PHB strain had a higher intracellular NADH/NAD⁺ ratio compared to the EP, suggesting changes in the redox state with PHB synthesis (Supplementary Table S8). Production of acetate, the main native by-product of *C. autoethanogenum* metabolism (Abrini et al., 1994; Marcellin et al., 2016), decreased compared to the EP grown on syngas (p-value<0.01; two-tailed equal variance *t*-test) while no difference was observed on steel mill off-gas (Supplementary Table S8).

3.2 Higher supply of H₂ increases cellular PHB content

We have recently shown that higher supply of H₂ leads to increased production of reduced by-products (Valgepea et al., 2018) since H₂ serves as a source for the generation of additional reducing power. Therefore, we assumed that growth on syngas (containing 10 times more H₂ compared to steel mill off-gas, 20 vs 2%) would result in higher PHB production. Indeed, the PHB cellular content (PHB%; grams of PHB per gDCW) was ~1.8 fold higher on syngas ($0.45 \pm 0.04\%$) compared to steel mill off-gas ($0.25 \pm 0.02\%$) (Figure 1B and Table 1). The PHB%, PHB titre, and PHB productivity are shown in Table 1.

Table 1 Condition-dependent PHB production in *C. autoethanogenum* PHB strain chemostats at dilution rate $\sim 1 \text{ day}^{-1}$ grown on steel mill off-gas or syngas.

Experiment	Abbreviation	Biological replicate	PHB production		
			PHB% ^a	Titer ^b	Productivity ^c
Steel mill off-gas (2% H ₂)	PHB2	01	0.26	0.00120	4.99E-05
		02	0.23	0.00097	4.05E-05
Syngas (20% H ₂) “Control”	PHB20	01	0.49	0.00221	9.15E-05
		02	0.41	0.00185	7.70E-05
Syngas “C/N ratio”	PHBC/N	01	0.15	0.00064	2.65E-05
		02	0.11	0.00050	2.07E-05
Syngas “Low Biomass”	PHBLowB	01	0.84	0.00119	4.94E-05
		02	0.75	0.00111	4.61E-05
Syngas “pH5.5”	PHBpH5.5	01	5.58	0.02250	9.37E-04
		02	5.61	0.02704	1.13E-03

^aGrams of PHB per gram of dry cell weight

^bGrams per litre in culture broth

^cGrams per litre per hour in culture broth

Interestingly, transcriptome analysis again showed changes in expression of genes of the arginine deiminase pathway (CAETHG_3021-22, arginine deiminase and ornithine carbamoyltransferase respectively, ~2.8-fold higher in PHB2 vs. PHB20, q-value=0.02; Supplementary Table S9). Intracellular metabolome analysis indicated that the higher PHB content on syngas was linked to a higher NADPH/NADP⁺ ratio (1.3-fold higher in PHB20 vs. PHB2; p-value=0.03) (Figure 1C; Supplementary Table S8). It is important to note that PHB production is NADPH-dependent (Figure 1A).

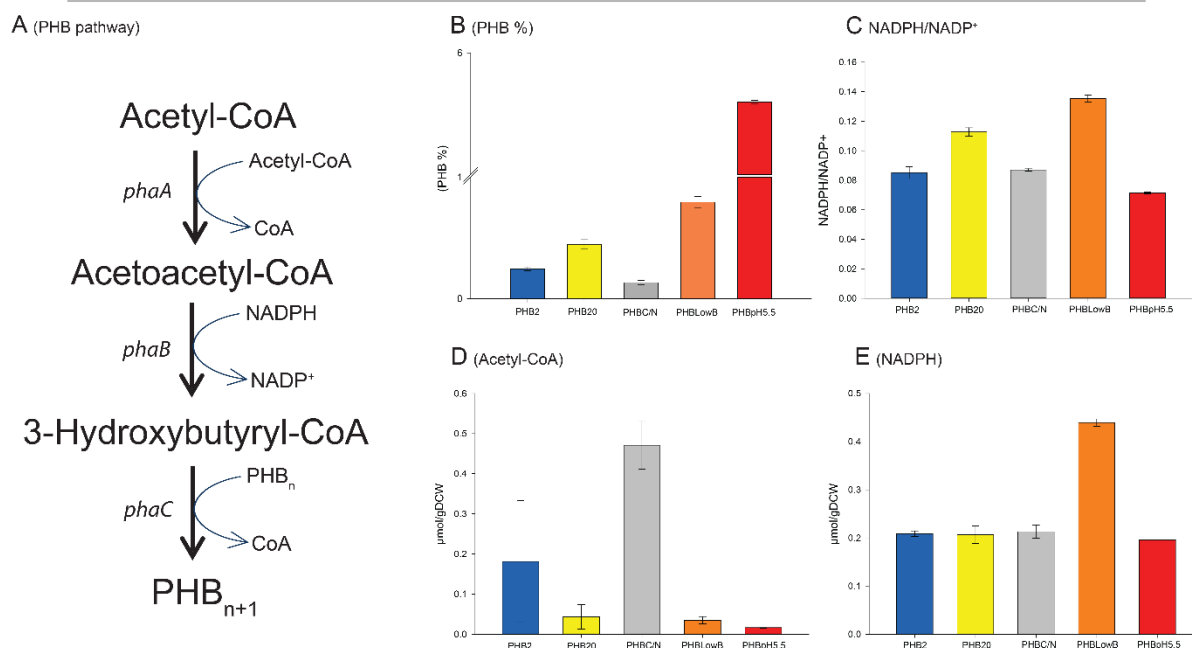


Figure 1 Condition-dependent cellular PHB and metabolite levels in the *C. autoethanogenum* PHB strain chemostats at a dilution rate of $\sim 1 \text{ day}^{-1}$. (A) The PHB pathway engineered into *C. autoethanogenum* is NADPH-dependent and comprises three genes/reactions from acetyl-CoA: 1) *phaA* (encoding a 3-ketothiolase enzyme that condenses two molecules of acetyl-CoA to form acetoacetyl-CoA, reaction “rxn00178_c0” in GEM); 2) *phaB* (encoding an NADPH-dependent acetoacetyl-CoA reductase that catalyses 3-hydroxybutyryl-CoA synthesis, “rxn01452_c0”); 3) *phaC* (encoding a PHA synthase that catalyses PHB polymerization, “PHB_polymer”). (B) Condition-dependent PHB cellular content (PHB%; grams of PHB per gDCW). (C) Condition-dependent NADPH/NADP⁺ ratio. (D) Condition-dependent acetyl-CoA concentration (μmol/gDCW). (E) Condition-dependent NADPH concentration (μmol/gDCW). Blue, yellow, gray, orange and red bars correspond to condition PHB2 (PHB strain grown on 2% H₂), PHB20 (growth on 20% H₂, “control”), PHBC/N (growth on 20% H₂, with C/N ratio increased 25x), PHBLowB (growth on 20% H₂, with 3x less biomass), and PHBpH5.5 (growth on 20% H₂, at pH5.5), respectively. Data represent average \pm standard error of two biological replicate chemostats.

3.3 Bioprocess engineering leads to increased PHB production

We next aimed to alter the cellular redox and energy states using bioprocess optimisation to examine the effect on PHB production. Compared to the control condition (PHB20, PHB% $0.45 \pm 0.06\%$), two hypotheses were tested. 1) Condition “PHBLowB”: because acetyl-CoA and NADPH pools increase at lower biomass concentrations (Valgepea et al., 2017a), we hypothesised that a lower steady-state biomass level would increase PHB production. 2) Condition “PHBpH5.5”: diffusion of acetic acid into the cell from the culture broth is lower at a higher pH, resulting in decreased uncoupling of the proton motive force (PMF) (Valgepea et al., 2017a). Therefore, we hypothesised that increasing the pH from 5 to 5.5 would drain less energy for maintaining the PMF. Consequently, lower demand for ATP could reduce acetate production, increasing the availability of acetyl-CoA for PHB production.

Both of our hypotheses were confirmed: PHB% increased in both the PHBLowB (~1.8 fold, p-value=0.03; PHB% $0.80 \pm 0.05\%$) and PHBpH5.5 (~12.5 fold, p-value<0.010; PHB% $5.60 \pm 0.02\%$) conditions compared to PHB20 (Figure 1B). Despite the increase achieved at pH 5.5, the PHB% of 5.6% is far from values reported for other organisms: 81.1% and 84% for *E. coli*; 73% for *Azotobacter beijerinckii*; and 70% for *Halomonas campaniensis*. These higher yields can potentially be explained by growth on sugar and at a more favourable pH for enzyme activities. Although, we could further enhance PHB production by increasing the pH to 6 (Supplementary Figure S1), the culture lost CO and H₂ uptake after one volume change at a dilution rate of 1 day⁻¹ (data not shown). Further experiments are needed to investigate the mechanisms responsible for increased PHB production at higher pH (e.g. beneficial for enzyme kinetics, lower drain of ATP for maintenance of PMF), and whether elevated PHB production at pH 6 could be maintained in continuous cultures.

3.3.1 Acetyl-CoA pool does not limit PHB production

Our hypothesis that higher pH could lead to elevated PHB production was confirmed (Figure 1B), but the intracellular acetyl-CoA pool was lower at pH 5.5 (Figure 1C). We then tested whether indeed the acetyl-CoA pool is not limiting PHB production in acetogens. It is known that in most native PHB-producing organisms, nitrogen limitation or a high C/N uptake ratio leads to higher PHB production through decreased demand for acetyl-CoA in other pathways (Du et al., 2001; Hong et al., 2003; Park and Lee, 1996; Peña et al., 2014). In other words, a higher fraction of the acetyl-CoA pool can be channelled into the PHB pathway under nitrogen limitation conditions. We thus hypothesised that increasing the C/N ratio (condition “PHBC/N”) in the culture feed could also lead to elevated PHB production in *C. autoethanogenum*. Surprisingly, despite the acetyl-CoA pool being 11 times higher (Figure 1D), the PHB% decreased ~3.4-fold (p-value=0.02) in PHBC/N ($0.13 \pm 0.02\%$) compared to PHB20 (Figure 1B).

3.3.2 Intracellular metabolomics highlights the importance of redox in heterologous production in acetogens

Elevated concentrations of acetyl-CoA did not correlate with increased PHB production. The fact that a significantly elevated acetyl-CoA pool in condition PHBC/N did not support increased PHB production (Figure 1B and 1D) may be explained by differences in the regulatory architectures between *C. autoethanogenum* and native PHB producers. Significant regulatory differences between native and heterologous PHB producers are reported (Koyama and Doi, 1995; Poblete-castro et al., 2012; Ramsay et al., 1990). Although increased pH (condition PHBpH5.5) supported greater PHB production, we could not identify obvious changes in the intracellular metabolome to explain this effect.

(Supplementary Table S8). However, we did observe a higher NADPH/NADP⁺ ratio (1.3-fold) in PHB20 and a higher NADPH pool (2.1-fold) in PHBLowB. These conditions resulted in greater PHB production than the PHB2 condition (Figure 1; Supplementary Table S8). In fact, the acetyl-CoA pool was lower in all conditions with a higher PHB% than PHB2 (Figure 1B and D). Our metabolome analysis showed no difference in the concentrations of WLP THF intermediates across the conditions, despite changes in acetyl-CoA and PHB levels (Supplementary Table S3). These results show that redox rather than the acetyl-CoA pool likely limits heterologous production in *C. autoethanogenum*.

3.3.3 Less CO₂ is produced in conditions with higher PHB (PHBLowB and PHBpH5.5)

Analysis of the carbon balance, and gas uptake and production rates (mmol/gDCW/h) are important for understanding the flow of carbon and to characterize energy and redox metabolism across conditions. Carbon recoveries for growth on syngas showed a deviation from 100% (average \pm standard error; PHB20 $89 \pm 0.6\%$; PHBC/N $108 \pm 9.2\%$; PHBLowB $104 \pm 0.2\%$; PHBpH5.5 $95 \pm 0.6\%$) within the range previously observed (Valgepea et al., 2017a), likely due to mass spectrometry off-gas analysis. Normalising carbon recoveries to 100% for a fair comparison of carbon balances between conditions first revealed that carbon incorporation into biomass varied very little despite differences in PHB% (Figure 2). Notably, carbon flow to CO₂ decreased in PHBLowB ($4 \pm 0.2\%$) and PHBpH5.5 ($17 \pm 1.6\%$) compared to PHB20 ($27 \pm 0.5\%$) (Figure 2), which is consistent with the lower CO₂ (q_{CO_2}) specific production rate for PHBLowB (1.01 ± 0.12 mmol/gDCW/h) and PHBpH5.5 (3.88 ± 0.37) compared to PHB20 (5.57 ± 0.13) (Table 2). Lower loss of substrate carbon as CO₂ is advantageous for a bioprocess both for increasing the carbon fixation and reducing greenhouse gas emissions. No statistically significant differences were seen in the CO (q_{CO}) and the H₂ (q_{H_2}) specific uptake rates (Table 2).

Both syngas conditions with higher PHB% also showed a decreased $q_{\text{CO}_2}/q_{\text{CO}}$ ratio (PHBLowB: 0.06 ± 0.01 and PHBpH5.5: 0.18 ± 0.01) compared to the PHB20 (0.26 ± 0.01). This suggests that the contribution of CO (from the oxidation to CO_2) to the reduction of ferredoxin (Fd_{red}) decreased. Interestingly, this observation was not accompanied by a concomitant increase in the $q_{\text{H}_2}/q_{\text{CO}}$ ratio (PHBLowB: 0.60 ± 0.01 ; PHBpH5.5: 0.56 ± 0.01 and PHB20: 0.55 ± 0.01), indicating that cells did not need to increase the production of reducing power from H_2 when less CO was oxidized (Bertsch and Müller, 2015; Schuchmann and Müller, 2014). No difference in the latter metrics was observed between PHBC/N and PHB20 (Figure 2; Supplementary Table S5).

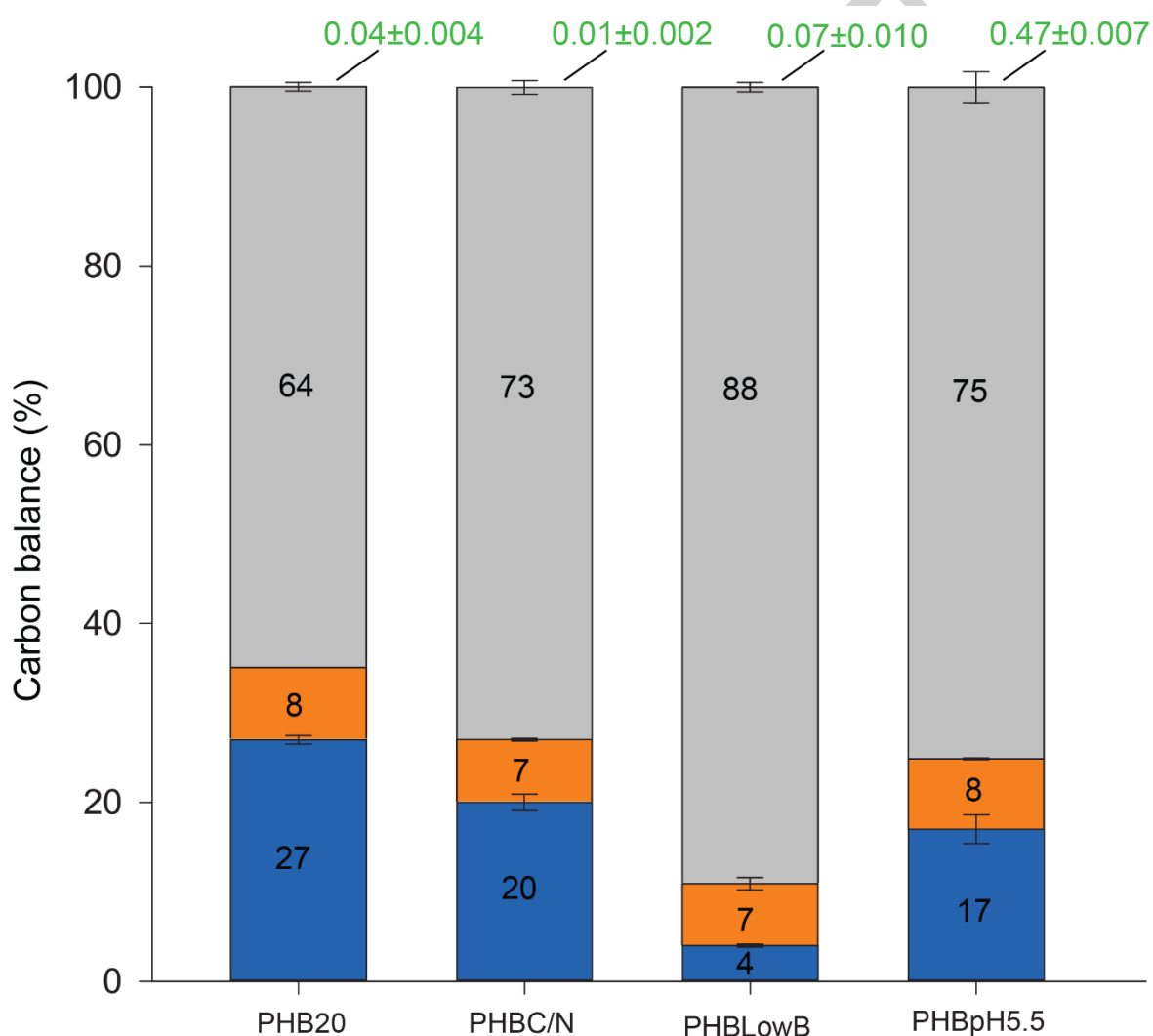


Figure 2 - Condition-dependent carbon balance in syngas-grown *C. autoethanogenum* PHB strain chemostats at a dilution rate of $\sim 1 \text{ day}^{-1}$. Carbon recoveries were normalized to 100%. Conditions: syngas (where gas data was available). Blue, orange, grey and green correspond to CO_2 , biomass, acetate and PHB, respectively. PHB20 (growth on 20% H_2 , “control”), PHBC/N (growth on 20% H_2 , with C/N ratio increased 25x), PHBLowB (growth on 20% H_2 , with 3x less biomass), and PHBpH5.5 (growth on 20% H_2 , at pH5.5). Data represent average \pm standard error of two biological replicate chemostats.

Table 2. Condition-dependent growth characteristics in syngas-grown *C. autoethanogenum* PHB strain chemostats at a dilution rate of $\sim 1 \text{ day}^{-1}$.

Experiment ^a	Abbreviation	Bio-replicate	BC ^b	Specific uptake rate ^c		Specific production rate ^c			Carbon recovery (%)
				q_{CO}	q_{H_2}	q_{CO_2}	q_{acetate}	q_{PHB}	
Syngas “Control”	PHB20	01	0.45	21.3	11.8	5.4	6.6	0.0023	81
		02	0.45	21.2	11.6	5.7	6.6	0.0020	81
Syngas “C/N ratio”	PHBC/N	01	0.42	18.5	12.8	4.3	8.5	0.0007	117
		02	0.45	22.7	12.3	4.9	8.6	0.0005	99
Syngas “Low Biomass”	PHBLowB	01	0.14	13.9	8.6	0.9	9.58	0.0041	103
		02	0.15	17.5	10.3	1.1	11.4	0.0036	104
Syngas “pH5.5”	PHBpH5.5	01	0.40	21.2	12	3.5	8.9	0.0267	96
		02	0.48	22.0	12.3	4.2	8.4	0.0274	94

^aNo data for gas uptake or production is available for PHB2 because the steel mill off-gas mix contained nitrogen (not argon) that hinders reliable gas analysis using mass-spectrometry as nitrogen interferes with the MS signal of CO ;

^bbiomass concentration (gDCW/L);

^cin mmol/gDCW/h.

3.4 Analysis of PHB production using a genome-scale metabolic model

To further understand the effect of PHB production on metabolism we estimated intracellular metabolic flux patterns using a genome-scale metabolic model (GEM). The GEM was constrained using experimental data (see Materials and Methods) and

maximisation of ATP dissipation was used as the objective function in flux balance analysis (FBA) (Figure 3; Supplementary Tables S4-5 SIM1-8).

Flux simulations confirmed the result of the carbon balance analysis that less CO₂ was dissipated in the conditions with higher PHB (i.e. “Low biomass” and “pH5.5”). Additionally, as observed previously (Valgepea et al., 2017a), Our simulations also showed that CO₂ in the WLP was directly reduced to formate with H₂ by the electron-bifurcating hydrogenase-formate dehydrogenase (HytA-E/FdhA) enzyme complex (Wang et al., 2013). By avoiding net redox consumption, this offers an advantage over CO₂ reduction by the redox-consuming formate dehydrogenase. We also observed that in the PHB_{LowB} and PHB_{pH5.5} experiments (where a reduction of q_{CO_2}/q_{CO} was not accompanied by an increase of q_{H_2}/q_{CO}), Fd_{red} was balanced by either increasing or decreasing the flux to some key reactions, like the AOR (aldehyde ferredoxin oxidoreductase), the electron bifurcating Nfn transhydrogenase complex (Marcellin et al., 2016; Wang et al., 2013), and the methylene-THF reductase bifurcating reaction, compared to the control (PHB₂₀). Surprisingly, PHB₂₀ showed a lower maintenance ATP cost (mmol/gDCW/h) and lower maintenance ATP costs from total ATP production (mATP%) *in silico* compared to PHB_{pH5.5} (Figure 3; Supplementary Tables S4-5). This is in contrast to our aforementioned hypothesis that a higher pH could lead to lower maintenance costs (see above).

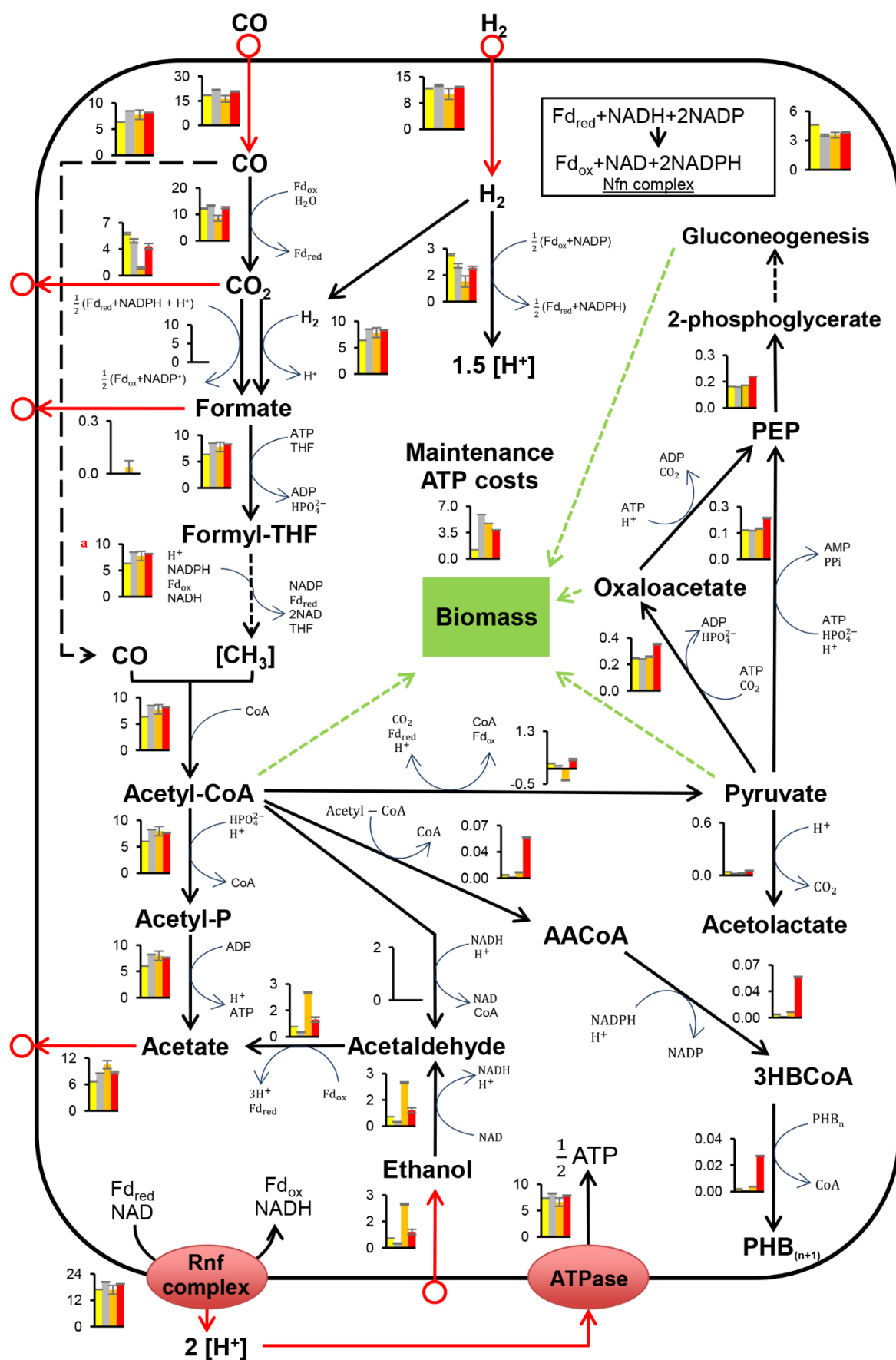


Figure 3 - Condition-dependent central metabolism fluxes in syngas-grown *C. autoethanogenum* PHB strain chemostats at a dilution rate of $\sim 1 \text{ day}^{-1}$. Fluxes (mmol/gDCW/h) are represented as the average \pm standard error of two biological replicate chemostats. Arrows show the direction of calculated fluxes. Red arrow denotes uptake or secretion. Flux into PEP from OAA and pyruvate is merged. ^amethylene-THF reductase flux is shown. Refer to Supplementary Tables S4-5 for flux data; Table S6 for metabolite abbreviations. Yellow bars represent PHB20 (growth on 20% H₂, “control”), gray PHBC/N (growth on 20% H₂, with C/N ratio increased 25x), orange PHBLowB (growth on 20% H₂, with 3x less biomass), and red PHBpH5.5 (growth on 20% H₂, at pH5.5).

3.4.1 PHB production is limited by ATP

A GEM is also useful for understanding potential factors limiting growth or metabolite production (e.g. ATP, reducing equivalents). Therefore, we used our GEM to simulate if ATP, NADH, NADPH, or Fd_{red} could be limiting PHB production in acetogens. First, we performed simulations by only maximising the PHB yield in FBA calculations (Supplementary Tables S4-5 SIM9-16) and then additionally constrained each of the “limiting” candidates with a fixed uptake rate value of 2 mmol/gDCW/h (SIM17-48) (see Materials and Methods for details). Our “single limitation” simulations yielded the highest PHB production (mmol/gDCW/h) with extra ATP supply across all tested conditions (PHB20, PHB C/N, PHBLowB, and PHB pH5.5). This observation is consistent with the understanding of acetogen metabolism being ATP-limited (Schuchmann and Müller, 2014). Simulations also showed that after ATP, Fd_{red}, NADPH, and then NADH availability potentially limit PHB production (Figure 4).

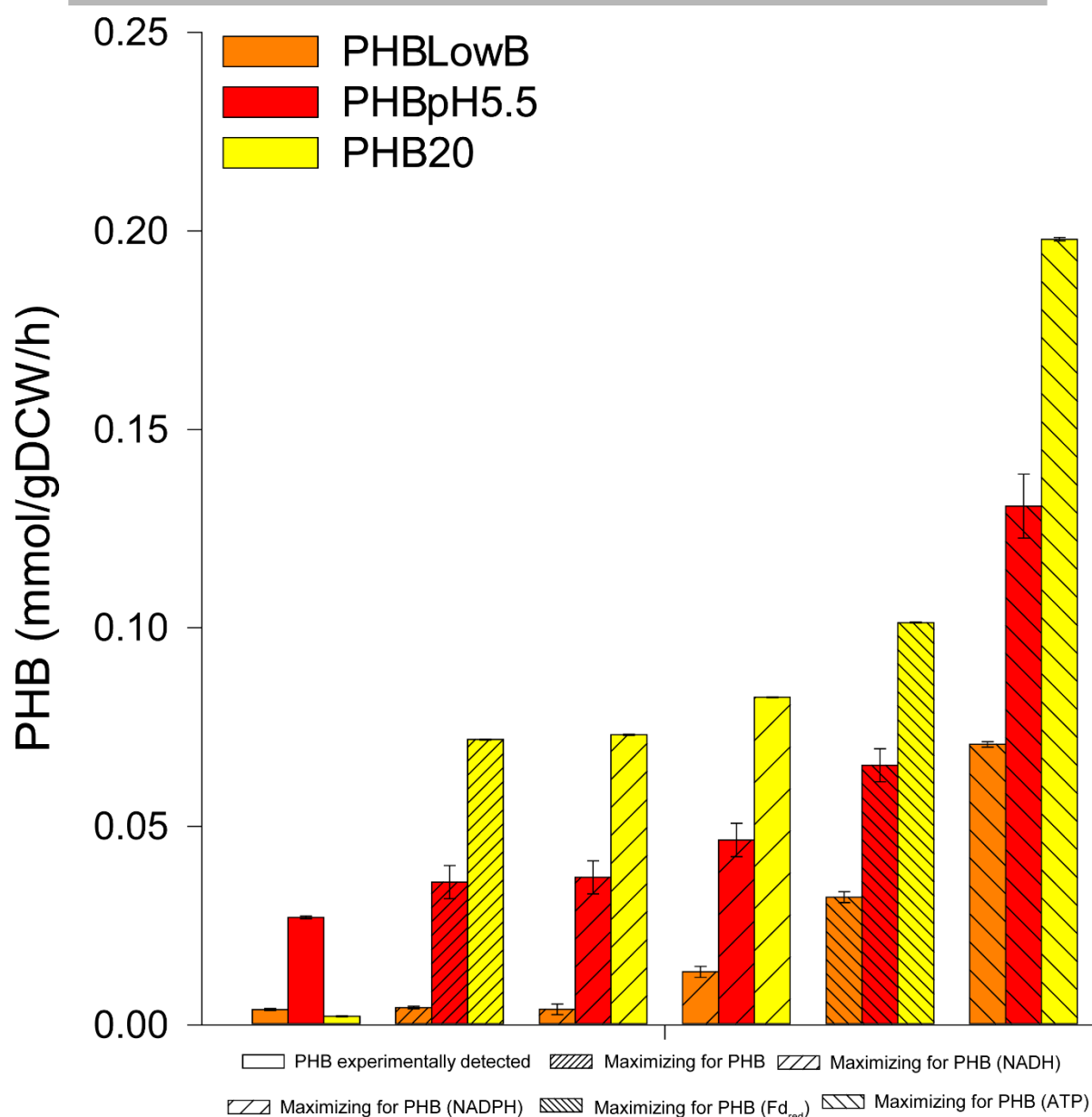


Figure 4 – Effect of cofactors on PHB production in the “single limitation” simulations using the GEM. PHB experimentally detected values from Figure 1B. Predicted maximal PHB production (mmol/gDCW/h) based on experimental data (“Maximising for PHB”; “control”) and with additional supply (2mmol/gDCW/h) of either NADH, NADPH, Fd_{red}, or ATP (“single limitation”) using the GEM. PHB20 (growth on 20% H₂, “control”), PHBLowB (growth on 20% H₂, with 3x less biomass), and PHBpH5.5 (growth on 20% H₂, at pH5.5). Data represent an average ± standard error of two biological replicate chemostats.

Lastly, we tested which paired cofactor combination together with ATP could improve PHB production further (SIM49-72). These double limitation simulations showed the strongest effect by ATP-Fd_{red}, followed by ATP-NADPH, and then ATP-NADH (Supplementary Figure S2), consistent with the trend found for “single limitation” simulations (Figure 4). These results confirm the importance of ATP and Fd_{red} as high energy carriers in acetogens. ATP mostly supports anabolism and cellular maintenance, Fd_{red} is essential for the Rnf energy conservation complex (Biegel et al., 2011) and only Fd_{red} is known to provide electrons for the reduction of CO₂ to CO in the carbonyl branch of the WLP (Schuchmann and Müller, 2014).

4. Discussion

A variety of relevant fuels and chemicals can potentially be produced from gas fermentation through heterologous production in acetogens (Cueto-Rojas et al., 2015; Liew et al., 2016). However, innate ATP and redox limitations in acetogen metabolism have to be overcome to expand beyond their native products (Molitor et al., 2017; Schuchmann and Müller, 2014). With the advent of genetic tools, genome-scale metabolics models and -omics workflows, an increasing number of studies are helping to shed light on the regulation of acetogen metabolism, especially on its autotrophic metabolism (Leang et al., 2013; Liew et al., 2017; Marcellin et al., 2016; Molitor et al., 2016; Valgepea et al., 2018, 2017a). Here, we explored acetogen metabolism further with a recombinant strain producing PHB to understand how acetogens can be used as cell factories for the production of industrially relevant compounds. This is the first work to report production of PHB in a gas-fermenting acetogen, exemplifying the versatility of this metabolic platform.

Although PHB production is not directly ATP-dependent (Figure 1A), *in silico* simulations revealed that extra ATP is needed to enhance PHB production, likely because cells natively prefer to convert acetyl-CoA into acetate (yielding ATP) rather than PHB. ATP availability is believed to constrain acetogen metabolism (Molitor et al., 2017; Schuchmann and Müller, 2014) and strategies are needed to overcome this limitation when using acetogens as cell factories. Here, we achieved the highest cellular PHB content by increasing the pH of the culture (Figure 1B). We hypothesised that this could arise from a more favourable energy state due to diminished uncoupling of the PMF from lower diffusion of acetic acid into the cell at a higher pH (Valgepea et al., 2017a). pH strongly influences the distribution of consumed carbon, and is linked to the shift between acetogenesis and solventogenesis (i.e. ethanol production) (Abubackar et al., 2016; Cotter et al., 2009; Klasson et al., 1993; Martin et al., 2015). These results suggest that both bioengineering and bioprocess optimisation are needed to construct robust cellular chassis with sufficient ATP supply for the production of heterologous products using gas fermentation. Complementary approaches, such as optimising the functional pH range of the heterologous enzymes, may provide equally beneficial effects on heterologous production.

Our results indicate that PHB production in acetogens is limited by redox rather than by the acetyl-CoA pool as higher PHB production was associated with an increased NADPH/NADP⁺ ratio and NADPH pool under some conditions with concomitantly lower acetyl-CoA levels (Figure 1). In addition to being the end product of the WLP, acetyl-CoA is a precursor metabolite for the synthesis of many potential bioproducts (e.g. production of butanol, butyrate, acetone, isopropanol, isoprene, bioplastics) (Bertsch and Müller, 2015; Liew et al., 2016). The acetyl-CoA pool might become limiting for the production of products other than PHB as significant changes in acetyl-CoA levels are reported between culture conditions (Amador-Noguez et al., 2011; Valgepea et al., 2017a).

The non-limiting acetyl-CoA pool for PHB production is somewhat surprising, although redox is already known to be an important factor governing product formation in acetogens (Marcellin et al., 2016; Valgepea et al., 2018, 2017a). These factors should be taken into account when designing strategies for the production of non-native products in acetogens.

Other strategies that can contribute to overcoming limitations of acetogen metabolism include changing the cofactor specificity from NADPH to NADH in key reactions. For instance, changing the cofactor of the acetoacetyl-CoA reductase from NADPH to NADH could increase PHB production, or any other downstream product from 3-hydroxybutyryl-CoA (e.g. butyrate, butanol). This could be achieved by introducing the PHB biosynthetic pathway from *Rhodospirillum rubrum* into acetogens. The *R. rubrum* pathway employs an NADH-dependent reductase to reduce acetoacetyl-CoA to (S)-3-hydroxybutyryl-CoA, which is then converted to (R)-3-hydroxybutyryl-CoA by two additional reactions that do not consume NADPH (Moskowitz and Merrick, 1969; Steinbüchel and Schlegel, 1991). These strategies are not specific for PHB production and can be explored for other products.

Re-distribution of carbon in acetogens can also be achieved by using different feed gas compositions (Valgepea et al., 2018), external electron supply by microbial electrosynthesis (Kracke et al., 2018, 2016), different media formulations (Abubackar et al., 2015, 2012; Valgepea et al., 2017b), or use of CRISPR interference (CRISPRi) (Woolston et al., 2018). Other promising routes for gas fermentation-based bioprocesses are coupling distinct pathways (e.g. PHB and β -oxidation pathways) and using two-stage bioprocesses either with co-cultures or integrating autotrophs and heterotrophs (Angenent et al., 2016; Claassens et al., 2016; Diender et al., 2016; Hu et al., 2016; Liew et al., 2016; Müller et al., 2013; Richter et al., 2016). Further work is needed to study the effects of any of these strategies on heterologous production using acetogens.

Conclusion

Our study shows, for the first time, PHB production using a gas-fermenting acetogen, *C. autoethanogenum*. We observed that the redox state of the cell rather than the acetyl-CoA pool limits heterologous production in *C. autoethanogenum*. Metabolic modelling, however, suggested that ultimately PHB production is potentially limited by ATP. Altogether, we advance the understanding of how acetogens, as cell factories, can be used to produce compounds outside their native by-products using gas fermentation.

Acknowledgements

We thank Terra Stark for the help with the intracellular metabolomics analysis. We thank Vishnuvardhan Mahamkali for help with model simulations. Elements of this research utilised equipment and support provided by the QLD nodes of BPA (metabolomics and Proteomics nodes) and the National Biologics Facility (www.nationalbiologicsfacility.com), an initiative of the Australian Government being conducted as part of the NCRIS National Research Infrastructure for Australia.

Declaration of interest

LanzaTech has interest in commercial gas fermentation with *C. autoethanogenum*. The authors have filed a provisional patent application based on the methods and results described here: (Lemgruber RSP, Valgepea K, Köpke M, Tappel R, Behrendorff J, Marcellin E, Nielsen LK. "Production of polyhydroxybutyrate in Wood-Ljungdahl microorganisms." United States Provisional Patent Application No. 62/568,127. October 4, 2017.)

Funding

This work was funded by the Australian Research Council (ARC LP140100213) in collaboration with LanzaTech. The ARC had no role in study design, data collection and

interpretation, or the decision to submit the work for publication. This research used equipment from the Queensland node of Metabolomics Australia, a National Collaborative Research Infrastructure (NCRIS) funded facility. We thank the following investors in LanzaTech's technology: BASF, CICC Growth Capital Fund I, CITIC Capital, Indian Oil Company, K1W1, Khosla Ventures, the Malaysian Life Sciences, Capital Fund, L. P., Mitsui, the New Zealand Superannuation Fund, Petronas Technology Ventures, Primetals, Qiming Venture Partners, Softbank China, and Suncor. KV acknowledges support from the European Union's Horizon 2020 research and innovation programme under grant agreement N°668997.

Availability of data and materials

RNA sequencing data has been deposited in the NCBI Gene Expression Omnibus depository under accession number GSE115837.

Supplementary material

Supplementary File 1. Supplementary Tables: Results of RNA-sequencing, metabolomics, and genome-scale modelling.

Supplementary File 2. Genbank file of the empty plasmid (pMTL83157.gb).

Supplementary File 3. Genbank file of the PHB plasmid (pPHB.gb).

Supplementary File 4. R-script used for transcriptomics analysis.

Supplementary File 5. R-script used for metabolomics analysis.

Supplementary File 6. Genome-scale metabolic model with its accompanying simulation files.

Supplementary Figure 1. PHB cellular content in syngas-grown *C. autoethanogenum* PHB strain chemostats at a dilution rate of $\sim 1 \text{ day}^{-1}$ and pH 6. PHB% measured in two biological replicate (1 and 2) chemostats are shown. Samples for PHB analysis were collected right after the cultures had lost uptake of CO and H₂.

Supplementary Figure 2. Effect of cofactors on PHB production in both “single” and “double” limitation simulations using the GEM. Experimentally determined PHB values are compared to *in silico* predicted maximal PHB production based on experimental data; “Single limitation” simulations for ATP, NADH, NADPH and Fdred are compared to “double limitation” simulations of cofactors pairs of ATP and NADH, NADPH, or Fdred. PHB20 (growth on 20% H₂, “control”), PHBC/N (growth on 20% H₂, with 25x higher C/N ratio), PHBLowB (growth on 20% H₂, with 3x less biomass), and PHBpH5.5 (growth on 20% H₂, at pH5.5). Data are presented as average ± standard error of two biological replicate chemostats.

References

- Abrini, J., Naveau, H., Nyns, E.-J., 1994. *Clostridium autoethanogenum*, sp. nov., an anaerobic bacterium that produces ethanol from carbon monoxide. *Arch. Microbiol.* 161, 345–351. <https://doi.org/10.1007/bf00303591>
- Abubackar, H.N., Fernández-Naveira, Á., Veiga, M.C., Kennes, C., 2016. Impact of cyclic pH shifts on carbon monoxide fermentation to ethanol by *Clostridium autoethanogenum*. *Fuel* 178, 56–62. <https://doi.org/10.1016/j.fuel.2016.03.048>
- Abubackar, H.N., Veiga, M.C., Kennes, C., 2015. Carbon monoxide fermentation to ethanol by *Clostridium autoethanogenum* in a bioreactor with no accumulation of acetic acid. *Bioresour. Technol.* 186, 122–127. <https://doi.org/10.1016/j.biortech.2015.02.113>
- Abubackar, H.N., Veiga, M.C., Kennes, C., 2012. Biological conversion of carbon monoxide to ethanol: Effect of pH, gas pressure, reducing agent and yeast extract. *Bioresour. Technol.* 114, 518–522. <https://doi.org/10.1016/j.biortech.2012.03.027>
- Amador-Noguez, D., Brasg, I. a, Feng, X.-J., Roquet, N., Rabinowitz, J.D., 2011. Metabolome remodeling during the acidogenic-solventogenic transition in *Clostridium*

acetobutylicum. Appl. Environ. Microbiol. 77, 7984–97.

<https://doi.org/10.1128/AEM.05374-11>

Angenent, L.T., Richter, H., Buckel, W., Spirito, C.M., Steinbusch, K.J.J., Plugge, C.M.,

Strik, D.P.B.T.B., Grootsholten, T.I.M., Buisman, C.J.N., Hamelers, H.V.M., 2016.

Chain Elongation with Reactor Microbiomes: Open-Culture Biotechnology to Produce Biochemicals. Environ. Sci. Technol. 50, 2796–2810.

<https://doi.org/10.1021/acs.est.5b04847>

Bengelsdorf, F.R., Poehlein, A., Linder, S., Erz, C., Hummel, T., Hoffmeister, S., Daniel, R.,

Dürre, P., 2016. Industrial Acetogenic Biocatalysts: A Comparative Metabolic and

Genomic Analysis. Front. Microbiol. 7, 1–15. <https://doi.org/10.3389/fmicb.2016.01036>

Bertsch, J., Müller, V., 2015. Bioenergetic constraints for conversion of syngas to biofuels in

acetogenic bacteria. Biotechnol. Biofuels 8, 210. <https://doi.org/10.1186/s13068-015-0393-x>

Biegel, E., Schmidt, S., González, J.M., Müller, V., 2011. Biochemistry, evolution and

physiological function of the Rnf complex, a novel ion-motive electron transport complex in prokaryotes. Cell. Mol. Life Sci. 68, 613–634.

<https://doi.org/10.1007/s00018-010-0555-8>

Brown, S.D., Nagaraju, S., Utturkar, S., De Tissera, S., Segovia, S., Mitchell, W., Land,

M.L., Dassanayake, A., Köpke, M., 2014. Comparison of single-molecule sequencing and hybrid approaches for finishing the genome of *Clostridium autoethanogenum* and

analysis of CRISPR systems in industrial relevant Clostridia. Biotechnol. Biofuels 7, 40.

<https://doi.org/10.1186/1754-6834-7-40>

Claassens, N.J., Sousa, D.Z., dos Santos, V.A.P.M., de Vos, W.M., van der Oost, J., 2016.

Harnessing the power of microbial autotrophy. Nat. Rev. Microbiol. 14, 692–706.

<https://doi.org/10.1038/nrmicro.2016.130>

- Cotter, J.L., Chinn, M.S., Grunden, A.M., 2009. Influence of process parameters on growth of *Clostridium ljungdahlii* and *Clostridium autoethanogenum* on synthesis gas. *Enzyme Microb. Technol.* 44, 281–288. <https://doi.org/10.1016/j.enzmictec.2008.11.002>
- Cueto-Rojas, H.F., van Maris, A.J.A., Wahl, S.A., Heijnen, J.J., 2015. Thermodynamics-based design of microbial cell factories for anaerobic product formation. *Trends Biotechnol.* 33, 534–546. <https://doi.org/10.1016/j.tibtech.2015.06.010>
- Daniell, J., Köpke, M., Simpson, S., 2012. Commercial Biomass Syngas Fermentation. *Energies* 5, 5372–5417. <https://doi.org/10.3390/en5125372>
- De Livera, A.M., Dias, D.A., De Souza, D., Rupasinghe, T., Pyke, J., Tull, D., Roessner, U., McConville, M., Speed, T.P., 2012. Normalizing and integrating metabolomics data. *Anal. Chem.* 84, 10768–10776. <https://doi.org/10.1021/ac302748b>
- De Livera, A.M., Olshansky, M., Speed, T.P., 2013. Statistical Analysis of Metabolomics Data, in: Roessner, U., Dias, D.A. (Eds.), *Metabolomics Tools for Natural Product Discovery*. Humana Press, Totowa, NJ, pp. 291–307. https://doi.org/https://doi.org/10.1007/978-1-62703-577-4_20
- de Souza Pinto Lemgruber, R., Valgepea, K., Hodson, M.P., Tappel, R., Simpson, S.D., Köpke, M., Nielsen, L.K., Marcellin, E., 2018. Quantitative analysis of tetrahydrofolate metabolites from *Clostridium autoethanogenum*. *Metabolomics* 14, 35. <https://doi.org/10.1007/s11306-018-1331-2>
- Diender, M., Stams, A.J.M., Sousa, D.Z., 2016. Production of medium-chain fatty acids and higher alcohols by a synthetic co-culture grown on carbon monoxide or syngas. *Biotechnol. Biofuels* 9, 82. <https://doi.org/10.1186/s13068-016-0495-0>
- Drake, H.L., Küsel, K., Matthies, C., 2006. Acetogenic Prokaryotes, in: Dworkin, M., Rosenberg, E., Schleifer, K.H., Stackebrandt, E. (Eds.), *Prokaryotes (Ecophysiology and Biochemistry)*. Springer, New York, pp. 354–420.

- Du, G., Chen, J., Yu, J., Lun, S., 2001. Continuous production of poly-3-hydroxybutyrate by *Ralstonia eutropha* in a two-stage culture system. *J. Biotechnol.* 88, 59–65.
[https://doi.org/10.1016/S0168-1656\(01\)00266-8](https://doi.org/10.1016/S0168-1656(01)00266-8)
- Friedlingstein, P., Andrew, R.M., Rogelj, J., Peters, G.P., Canadell, J.G., Knutti, R., Luderer, G., Raupach, M.R., Schaeffer, M., Van Vuuren, D.P., Le Quere, C., 2014. Persistent growth of CO₂ emissions and implications for reaching climate targets. *Nat. Geosci.* 7, 709–715. <https://doi.org/10.1038/NGEO2248>
- Heap, J.T., Kuehne, S. a., Ehsaan, M., Cartman, S.T., Cooksley, C.M., Scott, J.C., Minton, N.P., 2010. The ClosTron: Mutagenesis in *Clostridium* refined and streamlined. *J. Microbiol. Methods* 80, 49–55. <https://doi.org/10.1016/j.mimet.2009.10.018>
- Heap, J.T., Pennington, O.J., Cartman, S.T., Carter, G.P., Minton, N.P., 2007. The ClosTron: A universal gene knock-out system for the genus *Clostridium*. *J. Microbiol. Methods* 70, 452–464. <https://doi.org/10.1016/j.mimet.2007.05.021>
- Heap, J.T., Pennington, O.J., Cartman, S.T., Minton, N.P., 2009. A modular system for *Clostridium* shuttle plasmids. *J. Microbiol. Methods* 78, 79–85.
<https://doi.org/10.1016/j.mimet.2009.05.004>
- Hess, V., Gallegos, R., Jones, J.A., Barquera, B., Malamy, M.H., Müller, V., 2016. Occurrence of ferredoxin:NAD⁺ oxidoreductase activity and its ion specificity in several Gram-positive and Gram-negative bacteria. *PeerJ* 4, e1515.
<https://doi.org/10.7717/peerj.1515>
- Hong, S.H., Park, S.J., Moon, S.Y., Park, J.P., Lee, S.Y., 2003. In silico prediction and validation of the importance of the Entner-Doudoroff pathway in poly(3-hydroxybutyrate) production by metabolically engineered *Escherichia coli*. *Biotechnol. Bioeng.* 83, 854–863. <https://doi.org/10.1002/bit.10733>
- Hu, P., Chakraborty, S., Kumar, A., Woolston, B.M., Liu, H., Emerson, D., Stephanopoulos,

- G., 2016. Integrated Bioprocess for Conversion of Gaseous Substrates to Liquids. *Proc. Natl. Acad. Sci. U. S. A.* 113, 3773–3778. <https://doi.org/10.1073/pnas.1516867113>
- Huang, H., Chai, C., Li, N., Rowe, P., Minton, N.P., Yang, S., Jiang, W., Gu, Y., 2016. CRISPR/Cas9-Based Efficient Genome Editing in *Clostridium ljungdahlii*, an Autotrophic Gas-Fermenting Bacterium. *ACS Synth. Biol.* 5, 1355–1361. <https://doi.org/10.1021/acssynbio.6b00044>
- Islam, M.A., Zengler, K., Edwards, E. a., Mahadevan, R., Stephanopoulos, G., 2015. Investigating *Moorella thermoacetica* Metabolism with a Genome-Scale Constraint-Based Metabolic Model. *Integr. Biol.* 7, 869–82. <https://doi.org/10.1039/C5IB00095E>
- Karr, D.B., Waters, J.K., Emerich, D.W., 1983. Analysis of Poly-beta-Hydroxybutyrate in *Rhizobium japonicum* Bacteroids by Ion-Exclusion High-Pressure Liquid Chromatography and UV Detection. *Appl. Environ. Microbiol.* 46, 1339–1344.
- Klasson, K.T., Ackerson, M.D., Clausen, E.C., Gaddy, J.L., 1993. Biological conversion of coal and coal-derived synthesis gas. *Fuel* 72, 1673–1678. [https://doi.org/10.1016/0016-2361\(93\)90354-5](https://doi.org/10.1016/0016-2361(93)90354-5)
- Köpke, M., Held, C., Hujer, S., Liesegang, H., Wiezer, A., Wollherr, A., Ehrenreich, A., Liebl, W., Gottschalk, G., Durre, P., 2010. *Clostridium ljungdahlii* represents a microbial production platform based on syngas. *Proc. Natl. Acad. Sci. U. S. A.* 107, 13087–13092. <https://doi.org/10.1073/pnas.1011320107>
- Koyama, N., Doi, Y., 1995. Continuous production of Poly(3-Hydroxybutyrate-Co-3-Hydroxyvalerate) by *Alcaligenes eutrophus*. *Biotechnol. Lett.* 17, 281–284.
- Kracke, F., Lai, B., Yu, S., Krömer, J.O., 2018. Balancing cellular redox metabolism in microbial electrosynthesis and electro fermentation – A chance for metabolic engineering. *Metab. Eng.* 45, 109–120. <https://doi.org/10.1016/j.ymben.2017.12.003>
- Kracke, F., Viridis, B., Bernhardt, P., Rabaey, K., Krömer, J.O., 2016. Redox dependent

- metabolic shift in *Clostridium autoethanogenum* by extracellular electron supply. *Biotechnol. Biofuels* 1–12. <https://doi.org/10.1186/s13068-016-0663-2>
- Leang, C., Ueki, T., Nevin, K.P., Lovley, D.R., 2013. A Genetic system for *Clostridium ljungdahlii*: A chassis for autotrophic production of biocommodities and a model homoacetogen. *Appl. Environ. Microbiol.* 79, 1102–1109. <https://doi.org/10.1128/AEM.02891-12>
- Liew, F., Henstra, A.M., Köpke, M., Winzer, K., Simpson, S.D., Minton, N.P., 2017. Metabolic Engineering of *Clostridium autoethanogenum* for Selective Alcohol Production. *Metab. Eng.* 40, 104–114. <https://doi.org/10.1016/j.ymben.2017.01.007>
- Liew, F., Martin, E., Tappel, R., Heijstra, B., Mihalcea, C., Köpke, M., 2016. Gas Fermentation – A Flexible Platform for Commercial Scale Production of Low Carbon Fuels and Chemicals from Waste and Renewable Feedstocks. *Front. Microbiol.* 7, 694. <https://doi.org/10.3389/fmicb.2016.00694>
- Livera, A.M. de, Bowne, J.B., 2014. *Metabolomics: Analysis of Metabolomics Data*. R package.
- Marcellin, E., Behrendorff, J.B., Nagaraju, S., DeTissera, S., Segovia, S., Palfreyman, R., Daniell, J., Licona-Cassani, C., Quek, L., Speight, R., Hodson, M.P., Simpson, S.D., Mitchell, W.P., Köpke, M., Nielsen, L.K., 2016. Low carbon fuels and commodity chemicals from waste gases – Systematic approach to understand energy metabolism in a model acetogen. *Green Chem.* 18, 3020–3028. <https://doi.org/10.1039/C5GC02708J>
- Martin, M.E., Richter, H., Saha, S., Angenent, L.T., 2015. Traits of selected *Clostridium* strains for syngas fermentation to ethanol. *Biotechnol. Bioeng.* 113, 531–539. <https://doi.org/10.1002/bit.25827>
- McGlade, C., Ekins, P., 2015. The geographical distribution of fossil fuels unused when limiting global warming to 2°C. *Nature* 517, 187–190.

<https://doi.org/10.1038/nature14016>

Molitor, B., Marcellin, E., Angenent, L.T., 2017. Overcoming the energetic limitations of syngas fermentation. *Curr. Opin. Chem. Biol.* 41, 84–92.

<https://doi.org/10.1016/j.cbpa.2017.10.003>

Molitor, B., Richter, H., Martin, M.E., Jensen, R.O., Juminaga, A., Mihalcea, C., Angenent, L.T., 2016. Carbon recovery by fermentation of CO-rich off gases - Turning steel mills into biorefineries. *Bioresour. Technol.* 215, 386–396.

<https://doi.org/10.1016/j.biortech.2016.03.094>

Moskowitz, G.J., Merrick, J.M., 1969. Metabolism of Poly- β -hydroxybutyrate. II. Enzymatic Synthesis of D-(-)- β -Hydroxybutyryl Coenzyme A by an Enoyl Hydrase from *Rhodospirillum rubrum*. *Biochemistry* 8, 2748–2755.

<https://doi.org/10.1021/bi00835a009>

Müller, J., MacEachran, D., Burd, H., Sathitsuksanoh, N., Bi, C., Yeh, Y.C., Lee, T.S., Hillson, N.J., Chhabra, S.R., Singer, S.W., Beller, H.R., 2013. Engineering of *Ralstonia eutropha* H16 for autotrophic and heterotrophic production of methyl ketones. *Appl. Environ. Microbiol.* 79, 4433–4439. <https://doi.org/10.1128/AEM.00973-13>

Munasinghe, P.C., Khanal, S.K., 2010. Biomass-derived syngas fermentation into biofuels. *Bioresour. Technol.* 101, 5013–5022. <https://doi.org/10.1016/B978-0-12-385099-7.00004-8>

Nagarajan, H., Sahin, M., Nogales, J., Latif, H., Lovley, D.R., Ebrahim, A., Zengler, K., 2013. Characterizing acetogenic metabolism using a genome-scale metabolic reconstruction of *Clostridium ljungdahlii*. *Microb. Cell Fact.* 12, 118. <https://doi.org/10.1186/1475-2859-12-118>

Park, J.S., Lee, Y.H., 1996. Metabolic characteristics of isocitrate dehydrogenase leaky mutant of *Alcaligenes eutrophus* and its utilization for poly-B-hydroxybutyrate

- production. J. Ferment. Bioeng. 81, 197–205. [https://doi.org/10.1016/0922-338X\(96\)82208-2](https://doi.org/10.1016/0922-338X(96)82208-2)
- Peña, C., Castillo, T., García, A., Millán, M., Segura, D., 2014. Biotechnological strategies to improve production of microbial poly-(3-hydroxybutyrate): a review of recent research work. Microb. Biotechnol. 7, 278–293. <https://doi.org/10.1111/1751-7915.12129>
- Peoples, O.P., Sinskey, A.J., 1989a. Poly- β -hydroxybutyrate biosynthesis in *Alcaligenes eutrophus* H16. Characterization of the genes encoding β -ketothiolase and acetoacetyl-CoA reductase. J. Biol. Chem. 264, 15293–15297.
- Peoples, O.P., Sinskey, A.J., 1989b. Poly- β -hydroxybutyrate (PHB) biosynthesis in *Alcaligenes eutrophus* H16. Identification and characterization of the PHB polymerase gene (phbC). J. Biol. Chem. 264, 15298–15303.
- Poblete-castro, I., Escapa, I.F., Jäger, C., Puchalka, J., Lam, C.M.C., Schomburg, D., Prieto, M.A., Santos, V.A.M. dos, 2012. The metabolic response of *P. putida* KT2442 producing high levels of polyhydroxyalkanoate under single- and multiple-nutrient-limited growth: Highlights from a multi-level omics approach. Microb. Cell Fact. 11, 34.
- Ragsdale, S.W., Pierce, E., 2008. Acetogenesis and the Wood-Ljungdahl pathway of CO₂ fixation. Biochim. Biophys. Acta 1784, 1873–1898. <https://doi.org/10.1016/j.bbapap.2008.08.012>
- Ramsay, B.A., Lomaliza, K., Chavarie, C., Dubé, B., Bataille, P., Ramsay, J.A., 1990. Production of poly-(beta-hydroxybutyric-co-beta-hydroxyvaleric) acids. Appl. Environ. Microbiol. 56, 2093–8. [https://doi.org/10.1016/S0922-338X\(97\)83009-7](https://doi.org/10.1016/S0922-338X(97)83009-7)
- Richter, H., Molitor, B., Diender, M., Sousa, D.Z., Angenent, L.T., 2016. A narrow pH range supports butanol, hexanol, and octanol production from syngas in a continuous co-culture of *Clostridium ljungdahlii* and *Clostridium kluyveri* with in-line product extraction. Front. Microbiol. 7, 1773. <https://doi.org/10.3389/fmicb.2016.01773>

- Schuchmann, K., Müller, V., 2014. Autotrophy at the thermodynamic limit of life: a model for energy conservation in acetogenic bacteria. *Nat. Rev. Microbiol.* 12, 809–821.
<https://doi.org/10.1038/nrmicro3365>
- Steinbüchel, A., Schlegel, H.G., 1991. Physiology and molecular genetics of poly(beta-hydroxyalkanoic acid) synthesis in *Alcaligenes eutrophus*. *Mol. Microbiol.* 5, 535–542.
- Tremblay, P., Zhang, T., Dar, S.A., Leang, C., Lovley, D.R., 2012. The Rnf Complex of *Clostridium ljungdahlii* Is a Proton-Translocating Ferredoxin:NAD⁺ Oxidoreductase Essential for Autotrophic Growth. *MBio* 4, e00406-12.
<https://doi.org/10.1128/mBio.00406-12>.Editor
- Valgepea, K., de Souza Pinto Lemgruber, R., Abdalla, T., Binos, S., Takemori, N., Takemori, A., Tanaka, Y., Tappel, R., Köpke, M., Simpson, S.D., Nielsen, L.K., Marcellin, E., 2018. H₂ drives metabolic rearrangements in gas-fermenting *Clostridium autoethanogenum*. *Biotechnol. Biofuels* 11, 55. <https://doi.org/10.1186/s13068-018-1052-9>
- Valgepea, K., de Souza Pinto Lemgruber, R., Meaghan, K., Palfreyman, R.W., Abdalla, T., Heijstra, B.D., Behrendorff, J.B., Tappel, R., Köpke, M., Simpson, S.D., Nielsen, L.K., Marcellin, E., 2017a. Maintenance of ATP Homeostasis Triggers Metabolic Shifts in Gas-Fermenting Acetogens. *Cell Syst.* 4, 505–515.
<https://doi.org/10.1016/j.cels.2017.04.008>
- Valgepea, K., Loi, K.Q., Behrendorff, J.B., de Souza Pinto Lemgruber, R., Plan, M., Hodson, M.P., Köpke, M., Nielsen, L.K., Marcellin, E., 2017b. Arginine deiminase pathway provides ATP and boosts growth of the gas-fermenting acetogen *Clostridium autoethanogenum*. *Metab. Eng.* 41, 202–211.
<https://doi.org/10.1016/j.ymben.2017.04.007>
- Vandamme, P., Coenye, T., 2004. Taxonomy of the genus *Cupriavidus*: A tale of lost and

found. Int. J. Syst. Evol. Microbiol. 54, 2285–2289. [https://doi.org/10.1099/ij.s.0.63247-](https://doi.org/10.1099/ij.s.0.63247-0)

0

- Wang, S., Huang, H., Kahnt, H.H., Mueller, A.P., Köpke, M., Thauer, R.K., 2013. NADP-Specific electron-bifurcating [FeFe]-hydrogenase in a functional complex with formate dehydrogenase in *Clostridium autoethanogenum* grown on CO. J. Bacteriol. 195, 4373–4386. <https://doi.org/10.1128/JB.00678-13>
- Wood, H.G., 1991. Life with CO or CO₂ and H₂ as a source of carbon and energy. FASEB J. 5, 156–163.
- Woolston, B.M., Emerson, D.F., Currie, D.H., Stephanopoulos, G., 2018. Rediverting carbon flux in *Clostridium ljungdahlii* using CRISPR interference (CRISPRi). Metab. Eng. 48, 243–253. <https://doi.org/10.1016/j.ymben.2018.06.006>

Highlights

- This paper describes the first heterologous systems level characterisation in continuous cultures of the gas fermenting *C. autoethanogenum*.
- Molecular characterisation shows that ATP limits heterologous production in acetogens metabolism.
- Intracellular redox as opposed to the acetyl-CoA pool limits heterologous PHB production in *C. autoethanogenum*.
- Understanding the redox and energy limitations resulted in a 12-fold increase in PHB production.